DR JAMES HARTWELL (Orcid ID : 0000-0001-5000-223X)
PROF. MICHAEL R R. BLATT (Orcid ID : 0000-0003-1361-4645)

Article type : MS - Regular Manuscript

CAM guard cell anion channel activity follows transcript abundance and is suppressed by apoplastic malate

Cécile Lefoulon[1], Susanna F. Boxall[2], James Hartwell[2], and Michael R. Blatt[1,3]

ORCID IDs: 0000-0002-1131-3710 (CL), 0000-0002-8753-101X (SFB), 0000-0001-5000-223X (JH), 0000-0003-1361-4645 (MRB)

[1]Laboratory of Plant Physiology and Biophysics, Bower Building, University of Glasgow, Glasgow G12 8QQ UK, and
[2]Department of Functional and Comparative Genomics, Institute of Integrative Biology, Biosciences Building, University of Liverpool, Crown Street, Liverpool L69 7ZB UK
[3]Correspondence to michael.blatt@glasgow.ac.uk, phone +44 (0)141 330 4771

Received: 13 April 2020
Accepted: 22 April 2020

Abstract

* Plants utilizing crassulacean acid metabolism (CAM) concentrate CO_2 around RuBisCO while reducing transpirational water loss associated with photosynthesis. Unlike stomata of C_3 and C_4 species, CAM stomata open at night for the mesophyll to fix CO_2 into malate (Mal) and store it in the vacuole. CAM plants decarboxylate Mal in the light, generating high CO_2 concentrations within the leaf behind closed stomata for refixation by RuBisCO.

* CO_2 may contribute to stomatal closure but additional mechanisms, plausibly including Mal activation of anion channels, ensure closure in the light.

* In the CAM species *Kalanchoë fedtschenkoi*, we found that guard cell anion channel activity, recorded under voltage clamp, follows *KfSLAC1* and *KfALMT12* transcript abundance, declining to near-zero by the end of the light period. Unexpectedly, however, we found that extracellular Mal inhibited the anion current of *Kalanchoë* guard cells, both in wild-type and RNAi mutants with impaired Mal metabolism.

* We conclude that the diurnal cycle of anion channel gene transcription, rather than the physiological signal of Mal release, is a key factor in the inverted CAM stomatal cycle.

Keywords: guard cell anion channel / voltage clamp / circadian stomatal regulation / crassulacean acid metabolism / malic acid metabolism / apoplast / *Kalanchoë fedtschenkoi*

Introduction

Stomata are pores that facilitate gas exchange across the largely impermeable cuticle of leaves and stems. They open and close in response to exogenous and endogenous signals and thereby control the exchange of gases, most importantly water vapour and CO_2, between the interior of the leaf and the atmosphere (Jezek & Blatt, 2017). Stomata exert major controls on the water and carbon cycles of the world and can limit photosynthetic rates by 50% or more when demand exceeds water supply (Lawson & Blatt, 2014; Franks *et al.*, 2017). Transpirational water loss through stomata is a key factor in the challenges of fresh water availability and crop production that are expected to unfold over the next 20-30 years (Franks *et al.*, 2017). Their activity is a critical determinant of water use efficiency (WUE), often defined as the amount of dry matter produced per unit of water transpired (Leakey *et al.*, 2019). Indeed, a very large body of data relates stomata, transpiration and carbon assimilation (Hetherington & Woodward, 2003; Lawson & Blatt, 2014), highlighting the trade-off between CO_2 availability and stomatal transpiration.

Guard cells surround the stomatal pore and regulate its aperture. They coordinate membrane transport through a complex network of intracellular signals to regulate solute flux, mainly of K^+, Cl^- and malate (Mal), and drive guard cell turgor (Hetherington & Woodward, 2003; Jezek & Blatt, 2017). Our deep knowledge of these processes has made the guard cell one of the best-known plant cell models for membrane transport, signalling and homeostasis. Several well-defined signals, including light and CO_2, affect ion transport to drive changes in water flux and alter cell volume, turgor and stomatal aperture. In most plants, light promotes stomatal opening by activating H^+-ATPases through a blue light-dependent signal cascade (Inoue & Kinoshita, 2017) leading to hyperpolarization of the plasma membrane. These changes in voltage engage inward-rectifying K^+ channels and H^+-coupled K^+ and Cl^- symporters to facilitate osmotic solute uptake (Jezek & Blatt, 2017) while suppressing anion channels at the plasma membrane (Roelfsema & Hedrich, 2005; Marten *et al.*, 2007; Ando & Kinoshita, 2018). Stomatal closure in the dark and at high partial pressures of CO_2 (pCO_2) is signalled through both Ca^{2+}-independent and Ca^{2+}-dependent pathways that inactivate inward-rectifying K^+ channels and activate outward-rectifying K^+ and Cl^- channels, including the SLAC1 and ALMT12 anion channels in Arabidopsis, to promote net osmotic solute loss (Blatt, 1990;

Lemtiri-Chlieh & MacRobbie, 1994; Brearley *et al.*, 1997; Grabov & Blatt, 1998; Grabov & Blatt, 1999; Marten *et al.*, 2007; Chen *et al.*, 2010; Jezek & Blatt, 2017).

Stomata of plants exhibiting Crassulacean Acid Metabolism (CAM) differ in their regulation from this norm. At the heart of CAM is a syndrome of metabolic and physiological adaptations that facilitate CO_2 concentration around RuBisCO while circumventing much of the water loss associated with gas exchange for photosynthesis (Hartwell *et al.*, 2016; Yang *et al.*, 2017). Compared with C_3 plants, CAM plants yield up to a 16-fold increase in WUE with little cost in assimilation (Borland *et al.*, 2009; Hartwell *et al.*, 2016), characteristics that underpin their adaptation to arid environments. They achieve these savings by initially fixing atmospheric CO_2 in the dark into Mal for storage in the mesophyll vacuole; they release and decarboxylate the stored Mal in the light for re-fixation by RuBisCO. CAM avoids futile cycling by temporal separation and optimization of primary and secondary CO_2 fixation via transcriptional, translational and post-translational control of key metabolic enzymes and transporters in the mesophyll (Hartwell, 2006; Abraham *et al.*, 2016; Boxall *et al.*, 2017; Yang *et al.*, 2017).

Significantly, CAM depends on a cycle of stomatal movement that is inverted relative to that of most other plants: CAM stomata open at night and close during the day, facilitating high pCO_2 within the leaf to favor its fixation by RuBisCO (Von Caemmerer & Griffiths, 2009; Owen & Griffiths, 2013). How CAM stomata achieve this inverted diurnal cycle remains a puzzle. During the daylight, CO_2 released with Mal breakdown is thought to promote stomatal closure; however, experimental manipulations of pCO_2 in *Kalanchoë* have suggested that stomatal closure in the daylight phase of the CAM cycle is mediated through means additional to that of high internal pCO_2 (Von Caemmerer & Griffiths, 2009). Furthermore, preventing nocturnal CO_2 fixation to malate, either by supplying leaves with pure nitrogen or CO_2-free air, or using transgenic mutants that lack key CAM enzymes, shows that CAM stomata continue to close at least partially in the light period, even in the absence of an internal supply of CO_2 normally afforded by the decarboxylation of malate in the mesophyll (Borland *et al.*, 1999; Von Caemmerer & Griffiths, 2009; Dever *et al.*, 2015; Boxall *et al.*, 2017).

One plausible factor promoting stomatal closure could be the activation of plasma membrane anion channels by daytime Mal loss from the mesophyll to the leaf apoplast. Such a mechanism would accord with evidence that the anion channels in guard cells of

some plants are enhanced by extracellular Mal (Hedrich & Marten, 1993; Hedrich *et al.*, 1994; Wang & Blatt, 2011; Mumm *et al.*, 2013), which may thus be an important factor in promoting anion efflux from the guard cells and stomatal closure. However, until now this mechanism has not been examined in the guard cells of a CAM plant. Here we report that, in guard cells of the CAM species *Kalanchoë fedtschenkoi*, the anion current is not enhanced, but is suppressed by extracellular Mal. We find that the relative anion current amplitude during the diurnal cycle follows the pattern of transcript levels, declining to a minimum at the end of the daylight period. Furthermore, we show that CAM loss-of-function RNAi mutants of mitochondrial NAD malic enzyme (NAD-ME) and pyruvate orthophosphate dikinase (PPDK), which are altered in nocturnal Mal accumulation and its decarboxylation in the light (Dever *et al.*, 2015), exhibit anion currents similar to the wild-type plants. These, and additional findings lead us to conclude that Mal release from the mesophyll cannot serve as a metabolic signal in CAM stomatal control and that the diurnal cycle in gene transcription and turnover of the anion channels is vital for the temporal coordination of the CAM stomatal cycle.

Methods

Plant growth and tissue preparation

Kalanchoë fedtschenkoi Hamet et Perrier plants were propagated clonally on a mixture of John Innes no. 3 potting soil and perlite (70:30) at 22^{o}C and 60% relative humidity under 200 µmol $m^{-2}s^{-1}$ white light in a 16:8 h light:dark cycle. *NAD-ME* and *rPPDK1* RNAi mutant lines of *Kalanchoë fedtschenkoi* were generated as described previously (Dever *et al.*, 2015) and grown under the same conditions. For all experiments, epidermal tissue was taken from leaves at positions 6-8 leaf pairs below the apex corresponding to tissue fully matured and undergoing obligatory CAM (Dever *et al.*, 2015; Boxall *et al.*, 2017). Representative examples of gas exchange from these leaves of wild-type, *NAD-ME* and *rPPDK1* RNAi mutant lines of *Kalanchoë fedtschenkoi* will be found in Supplemental Figure S2 of Dever et al (2015). Epidermal peels were prepared from these leaves and mounted, much as described previously (Blatt, 1987a; Wang & Blatt, 2011). All operations were carried out on an Axiovert S100TV microscope (Zeiss, http://www.zeiss.com/) fitted with Nomarski differential interference contrast optics. Peels were preincubated for 1 h in 50 mM KCl and 5 mM MES titrated to pH 6.1 with KOH.

Measurements were conducted at 22°C in continuous flowing solutions controlled by a gravity-fed system at a rate of 20 chamber volumes min^{-1}. The standard perfusion medium contained 15 mM Tetraethylammonium chloride (TEA-Cl), 15 mM CsCl and 5 mM 2-(N-morpholino)propanesulphonic acid (MES), titrated with $Ca(OH)_2$ to a pH 6.1 ($[Ca^{2+}]$ = 1.2 mM). Malate (Mal) and other compounds were added and removed as indicated during the course of experiments. Thus, each guard cell served as its own control with tests against possible 'rundown' of the current over the course of each impalement. Surface areas and volumes of impaled guard cells were calculated assuming a spheroid geometry using Henry IV EP software (Glasgow University, http://www.psrg.org.uk). Chemicals were from Sigma Aldrich (Poole, UK) unless otherwise specified.

Electrophysiology and current analysis

Voltage clamp recordings were obtained using double-barrelled microelectrodes coated with paraffin to reduce capacitance and filled with 100 mM CsCl (pH 7.5) to block K^+ channel currents (Grabov *et al.*, 1997; Chen *et al.*, 2010). Microelectrodes were connected to amplifier headstages via 1 M KCl/Ag–AgCl half-cells, and a 1 M KCl agar bridge served as the reference electrode. Membrane voltage was typically clamped at +40 mV for 10 s to activate the anion current before stepping the voltage to values between +40 and -200 mV, much as described previously (Grabov *et al.*, 1997). Current and voltage were recorded at 2 kHz after filtering the current with an 8-pole Bessel filter set to a cut-off frequency of 0.5 kHz. Currents were analysed using Henry IV EP software and fitted by non-linear least-squares using SigmaPlot v.11.1 (Systat, London UK) as described before (Chen *et al.*, 2010; Wang & Blatt, 2011). Instantaneous and steady-state currents were determined at 20 ms and 10 s, respectively, into clamp steps following channel activation. Data are presented as means ±SE of *n* observations and differences validated post-hoc by ANOVA or Student's t test.

Epidermal Peel Sampling for RNA Isolation

Prior to sampling for leaf epidermal peels, plants were entrained for 7-days in a Snijders Microclima MC-1000 growth cabinet set to 12-h-light (450 µmoles m^{-2} s^{-1}), 25˚C, 60 % humidity/ 12-h-dark, 15˚C, 70 % humidity. Epidermal peel samples were isolated

from leaf pairs 6-8, which perform full CAM in the wild type (Boxall *et al.*, 2020). Peels were collected from individual clonal plants every 4 h over a 12-h-light/12-h-dark cycle (12:12 LD), starting at 00:00 when the lights came on. The epidermal peels were detached from the leaves using a "snap and peel action" that destroys >95% of the pavement cells and were immediately frozen in liquid nitrogen. Six leaves were peeled for each sample to obtain both upper and lower epidermis. Epidermal samples were stored at -80°C until use.

Total RNA isolation and RT-qPCR

Total RNA was isolated from 100 mg of frozen, ground leaf epidermal tissue using the Qiagen RNeasy kit (Qiagen, Germany) following the manufacturer's protocol with the addition of 13.5 µL 50 mg mL^{-1} PEG 20000 to the 450 µL RLC buffer used for each extraction. cDNA was synthesized from the total RNA using the Qiagen Quantitect RT kit according to the manufacturer's instructions (Qiagen, Germany). The resulting cDNA was diluted 1:4 with molecular biology grade water prior to use in RT-qPCR. Transcript levels were determined using the SensiFAST SYBR No Rox kit (Bioline) in an Agilent MX3005P qPCR System Cycler. The results for each target gene transcript of interest were normalized to the reference gene *THIOESTERASE/THIOL ESTER DEHYDRASE-ISOMERASE SUPERFAMILY PROTEIN* (*TEDI*; Kaladp0068s0118.1; Arabidopsis orthologue AT2G30720.1). Gene expression in a pool of RNA generated from epidermal peels from LP6 samples collected every 4 h over a 12-h-light/ 12-h-dark cycle was set to 1. Primer pairs for RT-qPCR analyses were as follows: *SLAC1* Kaladp0050s0214.1 (*SLAC1F GTACTTCTCGTCGCTAAAGGG; SLAC1R ACTCAAGTCTCCATTTCAGCG)* and *ALMT12* Kaladp0091s0013.1 *(ALMT12F GTGACATCGAAATCAATGTGAC; ALMT12R AAATGGGAAGGAGCCTGTTTC).*

Results

Kalanchoë exhibits a characteristic SLAC-like anion current

Stomata of *Kalanchoë* are comparable in size to those of *Vicia* and *Nicotiana*, making them attractive targets for microelectrode impalement once isolated in epidermal peels (Figure 1). For these studies, we peeled the mature leaves of *Kalanchoë*

fedtschenkoi, taken from leaves positioned at pairs six through eight below the shoot apex. At these positions, the leaves are known to be fully developed in CAM metabolism; they retain full CAM activity in isolation and show no appreciable plasticity in this activity (Borland *et al.*, 2009; Dever *et al.*, 2015; Boxall *et al.*, 2017). Representative examples of gas exchange from these leaves, and from leaves at the same positions in the *NAD-ME* and *rPPDK1* RNAi mutant lines of *Kalanchoë fedtschenkoi* employed below, will be found in Supplemental Figure S2 of Dever et al (2015). In every case, we found the guard cells to be easily impaled with multibarrelled microelectrodes when peels were mounted as described before for impalements (Blatt, 1987a; Grabov *et al.*, 1997; Chen *et al.*, 2010).

We used double-barrelled microelectrodes for two-electrode voltage clamp recording, pulled to yield tips equivalent to those described previously with tip resistances greater than 200 MΩ when filled with 200 mM K^+ acetate and measured in 10 mM KCl solution (Blatt, 1987b; Blatt & Armstrong, 1993). To analyse the *Kalanchoë* anion channels, the electrodes were filled with 100 mM CsCl. Additionally, all measurements were carried out under continuous superfusion of epidermal peels with bathing solution of 5 mM Ca^{2+}-MES buffer, pH 6.1, with additions of 15 mM CsCl and 15 mM tetraethylammonium chloride (TEA-Cl). The combination of the Cs^+ electrolyte with Cs^+ and TEA^+ in the bath ensured that all background K^+ channel current was blocked in *Nicotiana* and Arabidopsis (Grabov *et al.*, 1997; Chen *et al.*, 2010), and this was found to hold true also for *Kalanchoë* guard cells. The characteristics of *Kalanchoë* guard cell K^+ channels will be the subject of a later publication. All measurements reported here were carried out by adding and removing compounds by superfusion in the bath during the course of recordings. Thus, each cell served as its own control for each of the various experimental treatments.

On continuous superfusion with 15 mM CsCl and 15 mM TEA-Cl (30 mM Cl^-) in the bath, clamping the membrane to voltages of +30 to +40 mV yielded a slow-activating current that deactivated over periods of several seconds on stepping to voltages negative of 0 mV. Figure 2 shows both the instantaneous and steady-state currents recorded following 10-s steps to +40 mV to activate the current. A significant feature of the instantaneous current was its modest dependence on voltage (Figure 2A) which relaxed to a steep dependence in the steady-state (Figure 2B,C). The current also showed kinetics in deactivation with halftimes in the range of 1-3 s (Figure 2B). Fitting the steady-

state currents to a Boltzmann function (see Figure 2 legend) indicated a voltage dependence consistent with a channel gating charge of approximately 1 and a mid-point voltage near 0 mV (Figure 2D). All of these characteristics are similar to those reported previously for SLAC-like anion currents of *Vicia*, *Nicotiana* and for SLAC1 in Arabidopsis (Schroeder & Keller, 1992; Schwartz *et al.*, 1995; Grabov *et al.*, 1997; Roelfsema *et al.*, 2004; Geiger *et al.*, 2009; Chen *et al.*, 2010).

Analysis of the current relaxations on increasing Cl^- in the bath indicated a negative displacement of the apparent reversal voltage as expected for an anion permeant channel (Figure 2E), albeit with a sub-Nerstian dependence concentration suggesting that Cl^- is not the only pemeant ion. Many anion channels are equally, or more permeant to NO_3^- (Schmidt & Schroeder, 1994). Because the dominant current clearly was carried by anion passage out of the cell, we loaded guard cells by including $CsNO_3$ in the microelectrodes. In this case, we observed no difference in instantaneous current and only a modest shift to more negative voltages in the reversal voltage of the steady-state current (Supplemental Figure S1). This difference is less than reported for *Vicia* guard cells (Schmidt & Schroeder, 1994; Grabov *et al.*, 1997) and may reflect a lower relative conductance for NO_3^-. Additions of 20 µM of the anion channel blocker 5-nitro-2-(3-phenylpropyl-amino) benzoic acid (NPPB) to the bath during recordings eliminated the current (see Figure 2), and the current recovered on washing out the blocker from the superfusion medium (see Supplemental Figure S2) so precluding current rundown. Thus, we concluded that the current is carried by Cl^-- and NO_3^--permeable anion channels at the plasma membrane.

Kalanchoë anion channel activity follows transcript abundance during the daylight period

The diurnal CAM cycle is commonly divided between four phases (see Figure 3A). Phase I corresponds to the period of nocturnal stomatal opening when CO_2 is fixed by PEPC to form malic acid, which is then transported into the mesophyll vacuole. Phase II marks a shift to RuBisCO activity just after dawn when, for a brief period, CO_2 is fixed by both PEPC and RuBisCO. Phase III marks a long phase of malic acid decarboxylation and CO_2 concentration behind closed stomata that promotes its refixation by RuBisCO. Finally, Phase IV marks the end of the light period when stomata typically reopen (Luttge,

2004; Davis *et al.*, 2014). We recorded anion currents at intervals over 10 h spanning the light period into the beginning of the dark period, that is through Phase III to the beginning of Phase I. Current amplitudes quantified at -120 mV from over 50 independent experiments (Figure 3B) showed a clear trend and substantial anion current early in Phase III with a mean amplitude of -197±17 μA/cm² at -120 mV, declining over the daytime to a mean current amplitude at the beginning of Phase IV of -51±6 μA/cm² at the same voltage. Statistical differences were evident in measurements between time points in the first 6 h, those at 8 h and measurements taken thereafter up to 12 h into the diurnal cycle. At the beginning of Phase I the anion current was generally too small to resolve.

Throughout the period of measurements, the currents showed little evidence of a change in reversal voltage, consistent with a primary effect on the number of channels. Joint fittings yielded common values for the gating parameters $V_{1/2}$ and δ between data sets; only the maximum ensemble conductance G_{max} varied and, like the instantaneous current (Figure 3C), G_{max} decreased over the light period. We also challenged guard cells with 20 μM NPPB at intervals to confirm the identity of the current. In every case, the current was inhibited by the anion channel blocker (Figure 3D and Supplemental Figure S2). We cannot rule out more subtle alterations in gating control. Nevertheless, the lack of change in the key gating parameters of $V_{1/2}$, δ and the apparent reversal voltage, and the constant sensitivity to the anion channel blocker NPPB, all suggest that the intrinsic origin of the current did not vary over the diurnal cycle. The consistency in $V_{1/2}$ and δ, and the sensitivity to NPPB also discount any significant changes in distribution between any underlying subpopulations of ion channels over the diurnal period. Thus, we conclude that the primary effect of daytime period was on the mean current amplitude.

To assess the possible association of the current amplitude with gene expression, we examined the transcript abundance of the two main anion channel genes, *KfSLAC1* and *KfALMT12* (Boxall *et al.*, 2020). RNA was isolated using separated epidermal peels from leaf pairs 6-8 of wild-type *K. fedtschenkoi* to enrich for intact guard cells from CAM-performing leaves. We also examined the transcript abundance of *KfSLAC1* and *KfALMT12* in epidermal peels of the *Kalanchoë rNAD-ME1* and *rPPDK1* RNAi mutant lines (Dever *et al.*, 2015; Boxall *et al.*, 2017) with suppressed activities of mitochondrial NAD malic enzyme (NAD-ME) and pyruvate orthophosphate dikinase (PPDK). These enzymes play key roles in Mal decarboxylation in the light period during CAM.

Mitochondrial NAD-ME releases CO_2 and pyruvate from malate, and PPDK converts pyruvate to PEP, which is subsequently recycled through gluconeogenesis to starch. These mutants were previously shown to reduce Mal cycling by roughly 70% (Dever *et al.*, 2015). We reasoned that the current might track the relative transcript abundance if the current amplitude reflected a diurnal variation in anion channel transcription and translation. We also anticipated that a similar overall pattern in anion channel transcript abundance might be evident, even if Mal cycling was reduced in the *rNAD-ME1* and *rPPDK1* RNAi mutant lines.

In the wild type, we found that *KfSLAC1* transcript abundance peaked around dawn and declined steeply throughout the light period, reaching a minimum after 8-12 h of light (Figure 4, *above*). This temporal pattern was broadly followed in both *rNAD-ME1* and *rPPDK1* mutant lines, although the overall level of *KfSLAC1* transcript was marginally reduced in the *rPPDK1* and *rNAD-ME1* mutants. *KfALMT12* transcript levels also declined to a minimum 8 h into the light period in the wild type, and rose in the dark to a daily peak at 20:00, 4 h before dawn (Figure 4, *below*). *KfALMT12* transcript levels were roughly 20-50% higher in both *rNAD-ME1* and *rPPDK1* mutants relative to the wild type, although the differences were not substantial except at the 16 and 20 h timepoints (Figure 4, *below*). A direct comparison of transcript abundance and current amplitudes between the three genotypes is not meaningful for several reasons, which we return to below. Furthermore, we can anticipate some lag time between transcription and the appearance of the functional channels at their target membrane. Nonetheless, it is clear that in wild-type *Kalanchoë* and in the two metabolically-impaired mutants, the transcript abundance of the two main anion channel genes broadly anticipated the variation in the anion current activity recorded in vivo.

Kalanchoë guard cell anion channels are suppressed by extracellular malate

Activating guard cell anion channels is a vital component of the mechanism driving stomatal closure and, in several species, has been reported to be favoured by extracellular Mal (Hedrich & Marten, 1993; Hedrich *et al.*, 1994; Wang & Blatt, 2011; Mumm *et al.*, 2013). Because Phase III, which occupies the majority of the light period, is associated with substantial Mal release from the mesophyll vacuole for decarboxylation (Luttge, 2004; Davis *et al.*, 2014), we reasoned that some Mal might be lost to the

apoplast as the organic acid anion. If so, it could serve to enhance the anion channel activity of the *Kalanchoë* guard cells, thereby promoting stomatal closure.

To test this idea, we challenged the guard cells, adding 0.1-10 mM Mal outside by superfusion in the bath during experiments while recording the anion current under voltage clamp. Because impalements could generally be held for periods of 30-40 min only, trials were also carried out over two different time periods within Phase III of the CAM cycle. In every case (Figure 5 and Supplemental Figures S2 and S3), we found that adding Mal to the bath suppressed the anion current, notably at millimolar concentrations, while at 0.1 mM Mal we observed no appreciable change in the anion current. We also observed the current to recover when Mal was washed out of the bath (see Supplemental Figure S2), so discounting a general rundown of the current during recordings. The reduction in the anion current and conductance with Mal also argues against a major permeability of the channels to Mal. The effects of millimolar Mal were most evident in the first half of Phase III. Later in Phase III the current was much reduced, making quantification of any additional reductions in current with Mal difficult to assess. Regardless, it was clear that low millimolar Mal led to a suppression of the anion current, not its enhancement. Thus, we concluded that, in itself, Mal was not effective as a signal to enhance the guard cell anion current.

To validate this conclusion, we also examined the current in the *rNAD-ME1* and *rPPDK1* RNAi mutant lines (Dever *et al.*, 2015). We reasoned that one mechanism favouring stomatal opening in these mutant lines might be the reduced activity of the anion current. However, voltage clamp analysis of the guard cells showed anion currents in both mutant lines that were statistically equivalent to those observed in guard cells from wild-type plants; like the wild-type plants, the currents of the two RNAi lines showed a similar decline over the light period of the CAM cycle (Figure 6), consistent with the pattern of transcript abundance (Figure 3). Thus, we concluded that changes in extracellular Mal could not explain the elevated anion current during the daylight period of the CAM cycle and we return to this point below.

Discussion

CAM depends fundamentally on a diurnal cycle of stomatal movements that is inverted relative to that of C_3 and C_4 plants. CAM plants achieve substantial gains in water use efficiency through nocturnal stomatal opening and CO_2 capture when the driving force for transpiration is low, and through CO_2 release behind closed stomata during the day which elevates pCO_2 in the leaf to facilitate its fixation by RuBisCO in the light (Ting, 1985; Luttge, 2004; Davis *et al.*, 2014). In C_3 species, there is strong evidence demonstrating that elevated pCO_2 within the leaf promotes stomatal closure (Lawson & Blatt, 2014; Jezek & Blatt, 2017; Zhang *et al.*, 2018), but several studies have indicated that pCO_2 alone cannot explain CAM stomatal behaviour. Notably, Von Caemmerer & Griffiths (2009) observed that *Kalanchoë* stomata opened when pCO_2 was reduced in the dark and at the end of the light period, but they failed to respond to a decreased pCO_2 in the light, even when pCO_2 in the leaf was reduced experimentally.

We have asked whether anion channel activity follows transcript abundance for the orthologues of the two major anion channels associated with stomatal closure in Arabidopsis (Jezek & Blatt, 2017). Mal release to the apoplast from the mesophyll during the daylight period might act also as a signal between the mesophyll and guard cells for stomatal closure to help elevate pCO_2 within the leaf. A critical question in this case is whether the activity of the anion channels might be enhanced by extracellular Mal as has been reported in several non-CAM species. Our analysis for the guard cells of *Kalanchoë fedtschenkoi* yields three key observations. We found that (1) the anion current activity exhibited a pattern high activity early in the light that declined towards the end of the light period, consistent with the diurnal cycle of stomatal movements; (2) this variation in current activity followed the diurnal cycle of transcript abundance for the major anion channels in the *Kalanchoë* guard cells, especially the predominant *KfSLAC1*; (3) manipulating Mal accumulation in the dark and decarboxylation in the light with genetic mutants showed no substantial effect on the anion current; finally, (4) experimental additions of Mal in the apoplast, even at low millimolar concentrations, led to an inhibition in the anion current, not its enhancement. These findings demonstrate an unexpected sensitivity to external Mal in *Kalanchoë* guard cells that is opposite to that found for anion channels in non-CAM guard cells. They indicate that a mechanism of anion channel

stimulation by apoplastic Mal cannot explain the diurnal cycle of stomatal closure in *Kalanchoë* and that the variation in stomatal movements is likely to depend on the diurnal cycle of anion channel transcription and turnover.

Could apoplastic Mal signal stomatal closure in Kalanchoë?

There is good reason to suspect that the apoplast of CAM leaves might exhibit diurnal variations in apoplastic Mal content although, to our knowledge, there exist no direct measurements of Mal in the CAM leaf apoplast. Several anion channels of plant membranes, including those of CAM plants, are conductive for Mal (Keller *et al.*, 1989; Smith *et al.*, 1990; Iwaskaki *et al.*, 1992; Cheffings *et al.*, 1997; Kohler & Raschke, 2000; Hafke *et al.*, 2003; Meyer *et al.*, 2010; Medeiros *et al.*, 2016; Eisenach *et al.*, 2017) and there is evidence that Mal can be lost to the apoplast, at least from the guard cells of *Vicia* and *Commelina* during stomatal closure (Dittrich & Raschke, 1977; Van Kirk & Raschke, 1977; Van Kirk & Raschke, 1978). Micromolar to low millimolar concentrations of Mal have been identified in the leaf apoplast of several non-CAM, dicotyledonous species (Gabriel & Kesselmeier, 1999; Lopez-Millan *et al.*, 2000; Hedrich *et al.*, 2001; O'Leary *et al.*, 2016). Furthermore, we know that Mal is the most abundant metabolite that undergoes a substantial diurnal rhythm in the CAM mesophyll (Chen *et al.*, 2002). Thus, if Mal is found in the *Kalanchoë* leaf apoplast, we anticipated that it might well be elevated during the light period by loss across the mesophyll plasma membrane when Mal is released from the vacuole for decarboxylation.

The anion channels of guard cells of *Vicia, Nicotiana* and Arabidopsis have been the focus of many studies over the past three decades. All three species show very similar channel characteristics at the plasma membrane that divide between dominant, slowly-activating (S-type) and transient, rapidly-activating (R-type) currents (Keller *et al.*, 1989; Schroeder & Keller, 1992; Grabov *et al.*, 1997; Chen *et al.*, 2010; Wang & Blatt, 2011). In Arabidopsis, these currents are associated with the *SLAC1* and *ALMT12* ion channel genes, respectively, that provide major pathways for anion efflux and promote solute loss for stomatal closure (Jezek & Blatt, 2017).

Our findings highlight, in *Kalanchoë*, anion current characteristics that are quantitatively similar to those of the SLAC1-like channels of *Vicia, Nicotiana* and Arabidopsis (Keller *et al.*, 1989; Schroeder & Keller, 1992; Schmidt & Schroeder, 1994;

Grabov *et al.*, 1997; Chen *et al.*, 2010; Wang & Blatt, 2011). These characteristics extend to the voltage-dependent conductance of the current, its slow (de)activation kinetics, and Cl^- and NO_3^- permeabilities. Thus, both thermodynamic and kinetic considerations suggest that the *Kalanchoë* anion current is similarly important for solute efflux and stomatal closure.

The archetypal anion channels found in *Vicia*, tobacco and Arabidopsis are enhanced by low millimolar extracellular Mal (Hedrich & Marten, 1993; Wang & Blatt, 2011). Thus, we anticipated that Mal might well be important as a signal in *Kalanchoë* stomatal control. The critical question, therefore, was whether Mal affected the anion channels to promote their gating in *Kalanchoë* as it does in these other species. Surprisingly, unlike the anion channels found in *Vicia*, tobacco and Arabidopsis, the *Kalanchoë* anion current was not activated, but was reversibly inhibited by millimolar external Mal. This effect was evident throughout the light period. It was also clearly demonstrable earlier in Phase III of the light period when the activity of the channels would need to be highest to facilitate stomatal closure and when Mal release and its possible leakage from the mesophyll might be expected. In short, even if apoplastic Mal does increase during the daytime in *Kalanchoë* leaves, the enhanced activity of the guard cell anion current cannot be explained on the basis of its stimulation by Mal, because the action of the acid anion is to *suppress* the current.

Anion channel activity follows the daytime decline in transcript abundance

By contrast, we found that the transcript abundance of both the *Kalanchoë SLAC1* and *ALMT12* orthologues displayed a diurnal cycle that roughly approximated the temporal pattern for the anion current activities we were able to resolve. Notably, the *Kalanchoë SLAC1* transcript abundance rose during the night to a maximum at the start of the daylight period and declined steeply thereafter. This temporal pattern roughly matched the higher anion channel activity we recorded early in Phase III of the light period and its decline to near-zero values by Phase IV, at the end of the daylight period, when the stomata open. The *Kalanchoë ALMT12* transcript constituted a smaller proportion of transcript at all times throughout the diurnal cycle (Figure 4). Its abundance, too, showed a pronounced maximum, albeit roughly 4 h before the start of the daylight period.

We suspect that the earlier peak in *ALMT12* transcript anticipates the time, early in the daylight period, when anion channel activity is most important to promote stomatal closure. Accordingly, the 4-h gap between maximum *ALMT12* transcript abundance and the start of the daylight period may be seen to reflect a lag commensurate with mRNA processing and translation, and with anion channel assembly and delivery to the plasma membrane. A similar, 4-h temporal lag is known to occur between maximal *KfPPCK1* transcript abundance and KfPPCK-mediated PPC phosphorylation (Hartwell *et al.*, 1996; Hartwell *et al.*, 1999). In other words, a 4-h lag is a feature familiar among CAM transcriptional cycles and consistent with anticipation of the period of stomatal closure.

There is an additional reason to expect ALMT12 transcript abundance might preceed the time period in which the channel activity was most needed. In Arabidopsis, ALMT12 is associated with the fast-inactivating or Rapid (R-) type anion current, QUAC1 (Meyer *et al.*, 2010; Mumm *et al.*, 2013). A significant feature of the ALMT12 current is its voltage dependence, which ensures ALMT12 activation only when the membrane is depolarized. As a consequence, the channel protein may reside at the membrane in abundance in advance of the daylight period, but until the membrane depolarizes - such as might follow on a decline in H^+-ATPase activity and enhanced SLAC1 current - the ALMT12 channel will remain silent and will not contribute to the total membrane current at rest (Jezek & Blatt, 2017). Thus, again, *ALMT12* transcript abundance anticipates a period of high anion channel activity, but it does not indicate directly the timing of this period.

It is equally significant that we observed overall the same temporal pattern for both anion channel transcripts in the wild-type and in the *Kalanchoë rNAD-ME1* and *rPPDK1* RNAi mutant lines (Dever *et al.*, 2015). As in the wild-type, this pattern in the *Kalanchoë rNAD-ME1* and *rPPDK1* mutants and its parallel to the temporal decline in anion channel activities (Figure 6) adds support to the idea that it is the transcriptional cycle of these genes that drives the cycle in anion currents evident in *Kalanchoë*. These lines generate a reduced amount of Mal at dawn compared to the wild type, and Mal turnover in the light period is greatly reduced (Dever *et al.*, 2015). We stress here that comparisons within each genotype are informative whereas comparisons between the three genotypes are not. Indeed, it is not surprising that the anion currents recorded, for example in the *rPPDK1* mutant (Figure 6), might be similar to those of the wild-type *Kalanchoë* even if

KfALMT12 abundance was altered relative to the wild type (Figure 4). The *rNAD-ME1* and *rPPDK1* mutants are likely to have other effects on cellular homeostasis that impact on gene translation and/or channel regulation. For example, one might reasonably argue that, with the reduction in Mal accumulation and turnover, there is less Mal in the cytosol as well as less released to the apoplast and available for uptake by the guard cells. Any one of these factors, in turn, could influence post-translational control of the anion current and, as a result, moderate the current even if the total population of anion channels differs from that of the wild-type *Kalanchoë*. What is important is that the decline in anion current in the mutants follows qualitatively with transcript abundance and, again, argues against any role of apoplastic Mal in regulating *Kalanchoë* stomatal movements.

In conclusion, we find that the anion channel current of *Kalanchoë fedtschenkoi* guard cells exhibits many of the characteristics of the SLAC1 family of anion channels known in guard cells of *Vicia, Nicotiana* and Arabidopsis. The *Kalanchoë* anion current follows a diurnal pattern of activity consistent with variations in transcript abundance for the *SLAC1* orthologue. The current shows a high level of activity during the daylight period especially earlier in Phase III of the CAM cycle, consistent with a role in facilitating the closed state of the stomata during this time. Unlike the archetypical S-type channels, the *Kalanchoë* current is markedly suppressed by apoplastic Mal at low millimolar concentrations. These characteristics lead us to conclude that transcript availability for translation of the channel protein and its turnover is likely to determine the activity of the anion current in *Kalanchoë* guard cells and that apoplastic Mal is not a metabolic signal promoting the anion current for stomatal closure for CAM.

Acknowledgements: We thank Amparo Ruiz-Pardo for her support in plant care. This work was supported by the Biotechnology and Biological Sciences Research Council (UK) grants BB/N006909/1, BB/P011586/1 and BB/N01832X/1 to MRB.

Author contributions: CL and MB designed the experiments with JH; CL carried out the electrophysiological studies and analysed the results with MB; SB carried out the

transcriptional studies and analysed the results with JH; MB and CL wrote the manuscript with support from JH and SB

References

Abraham PE, Yin H, Borland AM, Weighill D, Lim SD, De Paoli HC, Engle N, Jones PC, Agh R, Weston DJ, et al. 2016. Transcript, protein and metabolite temporal dynamics in the CAM plant Agave. *Nature Plants* **2**(12).

Ando E, Kinoshita T. 2018. Red Light-Induced Phosphorylation of Plasma Membrane H+-ATPase in Stomatal Guard Cells. *Plant Physiology* **178**(2): 838-849.

Blatt MR. 1987a. Electrical characteristics of stomatal guard cells: the contribution of ATP-dependent, "electrogenic" transport revealed by current-voltage and difference-current-voltage analysis. *Journal Of Membrane Biology* **98**: 257-274.

Blatt MR. 1987b. Electrical characteristics of stomatal guard cells: the ionic basis of the membrane potential and the consequence of potassium chloride leakage from microelectrodes. *Planta* **170**: 272-287.

Blatt MR. 1990. Potassium channel currents in intact stomatal guard cells: rapid enhancement by abscisic acid. *Planta* **180**: 445-455.

Blatt MR, Armstrong F. 1993. K^+ channels of stomatal guard cells: abscisic acid-evoked control of the outward rectifier mediated by cytoplasmic pH. *Planta* **191**: 330-341.

Borland AM, Griffiths H, Hartwell J, Smith JAC. 2009. Exploiting the potential of plants with crassulacean acid metabolism for bioenergy production on marginal lands. *Journal Of Experimental Botany* **60**(10): 2879-2896.

Borland AM, Hartwell J, Jenkins GI, Wilkins MB, Nimmo HG. 1999. Metabolite control overrides circadian regulation of phosphoenolpyruvate carboxylase kinase and CO2 fixation in Crassulacean acid metabolism. *Plant Physiology* **121**(3): 889-896.

Boxall SF, Dever LV, Knerova J, Gould PD, Hartwell J. 2017. Phosphorylation of Phosphoenolpyruvate Carboxylase Is Essential for Maximal and Sustained Dark CO2 Fixation and Core Circadian Clock Operation in the Obligate Crassulacean Acid Metabolism Species Kalanchoe fedtschenkoi. *Plant Cell* **29**(10): 2519-2536.

Boxall SF, Kadu N, Dever LV, Knerova J, Waller J, Gould PJD, Hartwell J. 2020. Kalanchoë PPC1 is Essential for Crassulacean Acid Metabolism and the Regulation of Core Circadian Clock and Guard Cell Signaling Genes. *Plant Cell* **32**: 1136-1160.

Brearley J, Venis MA, Blatt MR. 1997. The effect of elevated CO_2 concentrations on K^+ and anion channels of Vicia faba L. guard cells. *Planta* **203**: 145-154.

Cheffings CM, Pantoja O, Ashcroft FM, Smith JAC. 1997. Malate transport and vacuolar ion channels in CAM plants. *Journal Of Experimental Botany* **48**: 623-631.

Chen LS, Lin Q, Nose A. 2002. A comparative study on diurnal changes in metabolite levels in the leaves of three crassulacean acid metabolism (CAM) species, Ananas comosus, Kalanchoe daigremontiana and K. pinnata *Journal Of Experimental Botany* **53**(367): 341-350.

Chen ZH, Hills A, Lim CK, Blatt MR. 2010. Dynamic regulation of guard cell anion channels by cytosolic free Ca^{2+} concentration and protein phosphorylation. *Plant Journal* **61**(5): 816-825.

Davis SC, LeBauer DS, Long SP. 2014. Light to liquid fuel: theoretical and realized energy conversion efficiency of plants using Crassulacean Acid Metabolism (CAM) in arid conditions. *Journal Of Experimental Botany* **65**(13): 3471-3478.

Dever LV, Boxall SF, Knerova J, Hartwell J. 2015. Transgenic Perturbation of the Decarboxylation Phase of Crassulacean Acid Metabolism Alters Physiology and Metabolism But Has Only a Small Effect on Growth. *Plant Physiology* **167**(1): 44-59.

Dittrich P, Raschke K. 1977. Malate metabolism in isolated epidermis of Commelina communis L. in relation to stomatal functioning. *Planta* **134**(1): 77-81.

Eisenach C, Baetz U, Huck NV, Zhang J, De Angeli A, Beckers GJM, Martinoia E. 2017. ABA-Induced Stomatal Closure Involves ALMT4, a Phosphorylation-Dependent Vacuolar Anion Channel of Arabidopsis. *Plant Cell* **29**(10): 2552-2569.

Franks PJ, Berry JA, Lombardozzi DL, Bonan GB. 2017. Stomatal Function across Temporal and Spatial Scales: Deep-Time Trends, Land-Atmosphere Coupling and Global Models. *Plant Physiol* **174**(2): 583-602.

Gabriel R, Kesselmeier J. 1999. Apoplastic solute concentrations of organic acids and mineral nutrients in the leaves of several fagaceae. *Plant and Cell Physiology* **40**(6): 604-612.

Geiger D, Scherzer S, Mumm P, Stange A, Marten I, Bauer H, Ache P, Matschi S, Liese A, Al-Rasheid KAS, et al. 2009. Activity of guard cell anion channel SLAC1

is controlled by drought-stress signaling kinase-phosphatase pair. *Proceedings Of The National Academy Of Sciences Of The United States Of America* **106**(50): 21425-21430.

Grabov A, Blatt MR. 1998. Membrane voltage initiates Ca^{2+} waves and potentiates Ca^{2+} increases with abscisic acid in stomatal guard cells. *Proceedings Of The National Academy Of Sciences Of The United States Of America* **95**: 4778-4783.

Grabov A, Blatt MR. 1999. A steep dependence of inward-rectifying potassium channels on cytosolic free calcium concentration increase evoked by hyperpolarization in guard cells. *Plant Physiology* **119**: 277-287.

Grabov A, Leung J, Giraudat J, Blatt MR. 1997. Alteration of anion channel kinetics in wild-type and abi1-1 transgenic Nicotiana benthamiana guard cells by abscisic acid. *Plant Journal* **12**: 203-213.

Hafke JB, Hafke Y, Smith JAC, Luttge U, Thiel G. 2003. Vacuolar malate uptake is mediated by an anion-selective inward rectifier. *Plant Journal* **35**(1): 116-128.

Hartwell J 2006. The circadian clock in CAM plants. In: Hall A, McWatters H eds. *Endogenour Rhythms in Plants*. Oxford: Blackwell, 211-236.

Hartwell J, Dever LV, Boxall SF. 2016. Emerging model systems for functional genomics analysis of Crassulacean acid metabolism. *Current Opinion In Plant Biology* **31**: 100-108.

Hartwell J, Gill A, Nimmo GA, Wilkins MB, Jenkins GL, Nimmo HG. 1999. Phosphoenolpyruvate carboxylase kinase is a novel protein kinase regulated at the level of expression. *Plant Journal* **20**(3): 333-342.

Hartwell J, Smith LH, Wilkins MB, Jenkins GI, Nimmo HG. 1996. Higher plant phosphoenolpyruvate carboxylase kinase is regulated at the level of translatable mRNA in response to light or a circadian rhythm. *Plant Journal* **10**(6): 1071-1078.

Hedrich R, Marten I. 1993. Malate-induced feedback regulation of plasma membrane anion channels could provide a CO_2 sensor to guard cells. *EMBO Journal* **12**: 897-901.

Hedrich R, Marten I, Lohse G, Dietrich P, Winter H, Lohaus G, Heldt HW. 1994. Malate-sensitive anion channels enable guard cells to sense changes in ambient CO_2 concentration. *Plant Journal* **6**: 741-748.

Hedrich R, Neimanis S, Savchenko G, Felle HH, Kaiser WM, Heber U. 2001. Changes in apoplastic pH and membrane potential in leaves in relation to stomatal responses to CO_2 , malate abscisic acid or interruption of water supply. *Planta* **213**(4): 594-601.

Hetherington AM, Woodward FI. 2003. The role of stomata in sensing and driving environmental change. *Nature* **424**(6951): 901-908.

Inoue S-i, Kinoshita T. 2017. Blue Light Regulation of Stomatal Opening and the Plasma Membrane H+-ATPase. *Plant Physiology* **174**(2): 531-538.

Iwaskaki I, Arata H, Kijima H, Nishimura M. 1992. Two types of channels involved in the malate ion transport across the tonoplast of a crassulacean acid metabolism plant. *Plant Physiology* **98**: 1494-1497.

Jezek M, Blatt MR. 2017. The Membrane Transport System of the Guard Cell and Its Integration for Stomatal Dynamics. *Plant Physiology* **174**(2): 487-519.

Keller BU, Hedrich R, Raschke K. 1989. Voltage-dependent anion channels in the plasma membrane of guard cells. *Nature* **341**: 450-453.

Kohler B, Raschke K. 2000. The delivery of salts to the xylem. Three types of anion conductance in the plasmalemma of the xylem parenchyma of roots of barley. *Plant Physiology* **122**(1): 243-254.

Lawson T, Blatt MR. 2014. Stomatal Size, Speed, and Responsiveness Impact on Photosynthesis and Water Use Efficiency. *Plant Physiology* **164**(4): 1556-1570.

Leakey ADB, Ferguson JN, Pignon CP, Wu A, Jin Z, Hammer GL, Lobell DB. 2019. Water Use Efficiency as a Constraint and Target for Improving the Resilience and Productivity of C3 and C4 Crops. *Annual Review of Plant Biology* **70**: 781-808.

Lemtiri-Chlieh F, MacRobbie EAC. 1994. Role of calcium in the modulation of Vicia guard cell potassium channels by abscisic acid: a patch-clamp study. *Journal Of Membrane Biology* **137**: 99-107.

Lopez-Millan AF, Morales F, Abadia A, Abadia J. 2000. Effects of iron deficiency on the composition of the leaf apoplastic fluid and xylem sap in sugar beet. Implications for iron and carbon transport. *Plant Physiology* **124**(2): 873-884.

Luttge U. 2004. Ecophysiology of Crassulacean Acid Metabolism (CAM). *Annals of Botany* **93**(6): 629-652.

Marten H, Hedrich R, Roelfsema MRG. 2007. Blue light inhibits guard cell plasma membrane anion channels in a phototropin-dependent manner. *Plant Journal* **50**(1): 29-39.

Medeiros DB, Martins SCV, Cavalcanti JHF, Daloso DM, Martinoia E, Nunes-Nesi A, DaMatta FM, Fernie AR, Araujo WL. 2016. Enhanced Photosynthesis and Growth in atquac1 Knockout Mutants Are Due to Altered Organic Acid Accumulation and an Increase in Both Stomatal and Mesophyll Conductance. *Plant Physiology* **170**(1): 86-101.

Meyer S, Mumm P, Imes D, Endler A, Weder B, Al-Rasheid KAS, Geiger D, Marten I, Martinoia E, Hedrich R. 2010. AtALMT12 represents an R-type anion channel required for stomatal movement in Arabidopsis guard cells. *Plant Journal* **63**(6): 1054-1062.

Mumm P, Imes D, Martinoia E, Al-Rasheid KAS, Geiger D, Marten I, Hedrich R. 2013. C-Terminus-Mediated Voltage Gating of Arabidopsis Guard Cell Anion Channel QUAC1. *Molecular Plant* **6**(5): 1550-1563.

O'Leary BM, Neale HC, Geilfus C-M, Jackson RW, Arnold DL, Preston GM. 2016. Early changes in apoplast composition associated with defence and disease in interactions between Phaseolus vulgaris and the halo blight pathogen Pseudomonas syringae Pv. phaseolicola. *Plant Cell And Environment* **39**(10): 2172-2184.

Owen NA, Griffiths H. 2013. A system dynamics model integrating physiology and biochemical regulation predicts extent of crassulacean acid metabolism (CAM) phases. *New Phytologist* **200**(4): 1116-1131.

Roelfsema MRG, Hedrich R. 2005. In the light of stomatal opening: new insights into 'the Watergate'. *New Phytologist* **167**(3): 665-691.

Roelfsema MRG, Levchenko V, Hedrich R. 2004. ABA depolarizes guard cells in intact plants, through a transient activation of R- and S-type anion channels. *Plant Journal* **37**(4): 578-588.

Schmidt C, Schroeder JI. 1994. Anion selectivity of slow anion channels in the plasma membrane of guard cells - large nitrate permeability. *Plant Physiology* **106**: 383-391.

Schroeder JI, Keller BU. 1992. Two types of anion channel currents in guard cells with distinct voltage regulation. *Proceedings Of The National Academy Of Sciences Of The United States Of America* **89**: 5025-5029.

Schwartz A, Ilan N, Schwarz M, Scheaffer J, Assmann SM, Schroeder JI. 1995. Anion channel blockers inhibit S-type anion channels and abscisic acid responses in guard cells. *Plant Physiology* **109**: 651-658.

Smith JAC, Pennington AJ, Martin RJ. 1990. A malate-specific ion channel in the vacuolar membrane of cam plants. *Plant Physiology* **93**: 32-32.

Ting IP. 1985. CRASSULACEAN ACID METABOLISM. *Annual Review Of Plant Physiology And Plant Molecular Biology* **36**: 595-622.

Van Kirk CA, Raschke K. 1977. Stomatal aperture and malate content of epidermis - effects of chloride and abscisic acid. *Plant Physiology* **59**(6): 96-108.

Van Kirk CA, Raschke K. 1978. Release of malate from epidermal strips during stomatal closure. *Plant Physiology* **61**(3): 474-475.

Von Caemmerer S, Griffiths H. 2009. Stomatal responses to CO2 during a diel Crassulacean acid metabolism cycle in Kalanchoe daigremontiana and Kalanchoe pinnata. *Plant Cell And Environment* **32**(5): 567-576.

Wang Y, Blatt MR. 2011. Anion channel sensitivity to cytosolic organic acids implicates a central role for oxaloacetate in integrating ion flux with metabolism in stomatal guard cells. *Biochemical Journal* **439**: 161-170.

Yang X, Hu R, Yin H, Jenkins J, Shu S, Tang H, Liu D, Weighill DA, Yim WC, Ha J, et al. 2017. The Kalanchoe genome provides insights into convergent evolution and building blocks of crassulacean acid metabolism. *Nature Communications* **8**.

Zhang J, De-oliveira-Ceciliato P, Takahashi Y, Schulze S, Dubeaux G, Hauser F, Azoulay-Shemer T, Toldsepp K, Kollist H, Rappel W-J, et al. 2018. Insights into the Molecular Mechanisms of CO2-Mediated Regulation of Stomatal Movements. *Current Biology* **28**(23): R1356-R1363.

Supporting Information

Figure S1. *Kalanchoë* anion currents are permeable to NO_3^-

Figure S2. *Kalanchoë* anion current suppression by Malate and block by the anion channel blocker 5-nitro-2-(3-phenylpropyl-amino) benzoic acid (NPPB) are reversible

Figure S3. *Kalanchoë* anion currents are inhibited by apoplastic malate (Mal)

Figure legends:

Figure 1. *Kalanchoë fedtschenkoi* stomatal complex.

Micrograph of a stomatal complex comprising a pair of guard cells with prominent chloroplasts in the center and three surrounding subsidiary cells. Image obtained using Nomarski differential interference contrast with a 40x objective. Scale bar, 15 μm.

Figure 2. *Kalanchoë fedtschenkoi* harbors anion channels with characteristics similar to those of SLAC1 in Arabidopsis

Mean instantaneous current-voltage (IV) relations (**A**) following 10-s activation of the current at +40 mV of at least 7 independent experiments were taken from the initial currents such as the examples shown in (**B**) across the voltage range between +40 and -180 mV. These currents relaxed to the mean steady-state curves (**C**) that showed little inward current, an apparent activation at voltages positive of -60 mV, and reversal voltages positive of 0 mV. We analyzed the mean steady-state IV curves using a Boltzmann function with an offset of the form

$$I = g_{max2}(V-E_x)+(g_{max1}(V-E_x))/(1+e^{\delta F/RT(V-V_{1/2})}) \quad [1]$$

where the total conductance was divided between g_{max1} as the voltage-dependent conductance maximum, and g_{max2} as the linear (voltage-independent) conductance maximum, E_x was the equilibrium (current reversal) voltage, $V_{1/2}$ was the voltage yielding half-maximal conductance for the voltage-sensitive component, δ was the corresponding voltage sensitivity coefficient describing the maximum slope of component conductance with voltage, and F, R and T have their usual meanings. Non-linear least-squares fittings (**D**) yielded common voltage-sensitivity of δ of 1.0± 0.04. $V_{1/2}$ values were -5±3, -7±2 and -

12±1 mV with 3, 15 and 30 mM Cl^- in the bath, respectively. Corresponding g_{max1} values were 0.4±0.01, 1.2±0.1 and 2.3±0.2 mS cm^{-2}, respectively. Tail current analysis showed a negative-going shift in the apparent E_x values as Cl^- increased (**E**), consistent with an anion conductance. Data are means ±SE of >7 independent experiments. Scale (**B**), 300 pA (vertical), 1 s (horizontal). Note that the symbols indicate measurements with bath solutions containing 3 (white circles), 15 (grey circles) and 30 mM (black circles) Cl^- in each case.

Figure 3. The *Kalanchoë* anion current declines throughout the daylight period of the CAM cycle

(**A**) The *Kalanchoë* CAM cycle is commonly divided between Phases I-IV as illustrated (refer to text for a description). Rc refers to the principle voltage clamp recording period. (**B**) Recordings were carried out throughout Phase III and IV to the beginning of Phase I and quantified as the mean instantaneous current recorded in 30 mM Cl^- at -120 mV from IV curves such as shown in (**C**) following a 10-s activation at +40 mV. Data are full scatter of measurements from >50 independent experiments (closed circles) where each data point represents the a single experiment and the mean of at least 3 measurements from one stomatal guard cell. Also shown are the means (open squares) binned at 1-h intervals with n>5 independent experiments within each bin. Each data point represents the means of at least 3 measurements from one stomatal guard cell. The solid curve is a non-linear least-squares fitting of the current values to a sigmoidal function and is included for visual reference. Letters above indicate statistical differences ($P<0.05$). (**C**) Instantaneous IV curves presented as means of >13 separate recordings at times between 4-6, 6-8 and 8-10 h. Data are cross-referenced to representative current traces in (**D**) by symbol. (**D**) Anion current sensitivity to 20 μM of the anion channel inhibitor 5-nitro-2-(3-phenylpropyl-amino) benzoic acid (NPPB) showed block independent of the daytime period. Here measurements were carried out (*top to bottom*) at times between 4-6 (closed squares), 6-8 (closed triangles) and 8-10 h (filled circles; see **A,C** above) and symbols cross-reference to the IV curves in (**C**). Scale: 400 pA (vertical), 1 s (horizontal). Representative data for NPPB washout are included in Supporting Information Figure S2.

Figure 4. Transcripts for the principal *Kalanchoë* guard cell anion channel genes *KfSLAC1* and *KfALMT12* decline throughout the daylight period to a minimum during Phase IV

Data are the means ±SE of six technical replicates for each of three independent experiments are for *KfSLAC1* (upper panel) and *KfALMT12* (lower panel) measured using RNA taken from wild-type *Kalanchoë* (closed circles) and from the *rNAD-ME1* (upright triangles) and *rPPDK1* mutant lines (inverted triangles). Data are plotted as a function time with the dark period indicated by the grey shading. Note that the 0 and 24 h timepoints are the same. Within each genotype, for *KfSLAC1*, data at 8, 12 and 16 h are significantly less than at the 0 (24), and 4 h timepoints; for *KfALMT12*, data at 16 and 20 h are significantly greater than at the 0 (24), 4, 8 and 12 h timepoints; in each case, for both transcripts, data at 0 (24) h is significantly greater than at 8 h ($P<0.05$).

Figure 5. *Kalanchoë* anion currents are inhibited by apoplastic malate (Mal)

Instantaneous current-voltage (IV) curves with the corresponding steady-state IV curves and maximum conductances (G_{max}) calculated as in Figure 2 (*upper insets*) for the time periods between 4-8 h (**A**) and 8-10 h (**B**). Representative current traces (*right inset*) are cross-referenced by symbol. Data are means ±SE of >6 independent experiments for each curve for 0 (black-filled symbols), 1 (grey-filled symbols) and 10 mM Mal (white symbols) added to the bath. Maximum conductances are included for additions of 0.1 mM Mal (see Supporting Information Figure S3) Letters indicate statistical differences at $P<0.05$. Scale: 400 pA (vertical), 1 s (horizontal). Representative data for Mal washout are included in Figure S2.

Figure 6. *Kalanchoë* anion currents in wild-type and the *rNAD-ME1* and *rPPDK1* mutants early and late in the daylight period

Instantaneous current-voltage (IV) curves (*left*) and the corresponding steady-state IV curves (*right*) for the time periods between 4-8 h (**A**) and 8-10 h (**B**). Data are means ±SE of >5 independent experiments for each curve for the wild type (black symbols), and two mutant lines of *rNAD-ME1* (white symbols) and for *rPPDK1* (grey symbols).

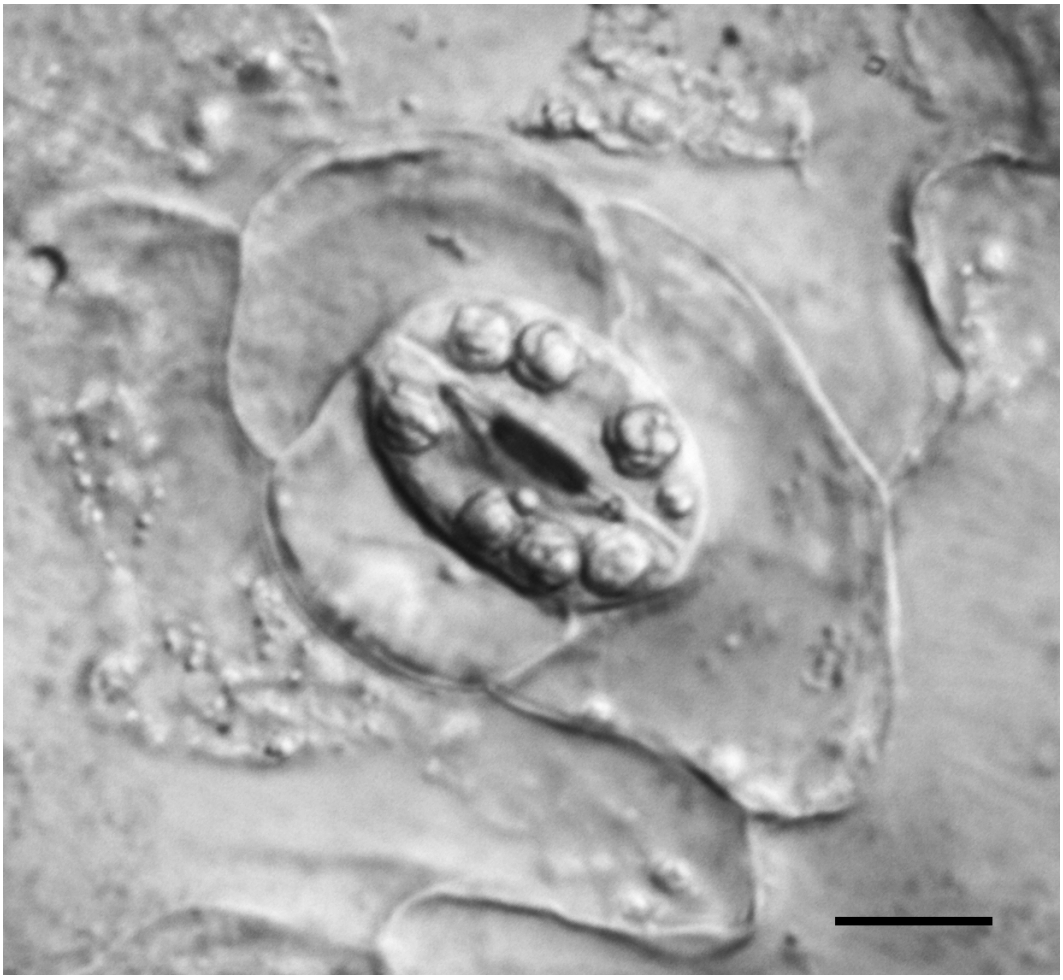

nph_16640_f1.jpg

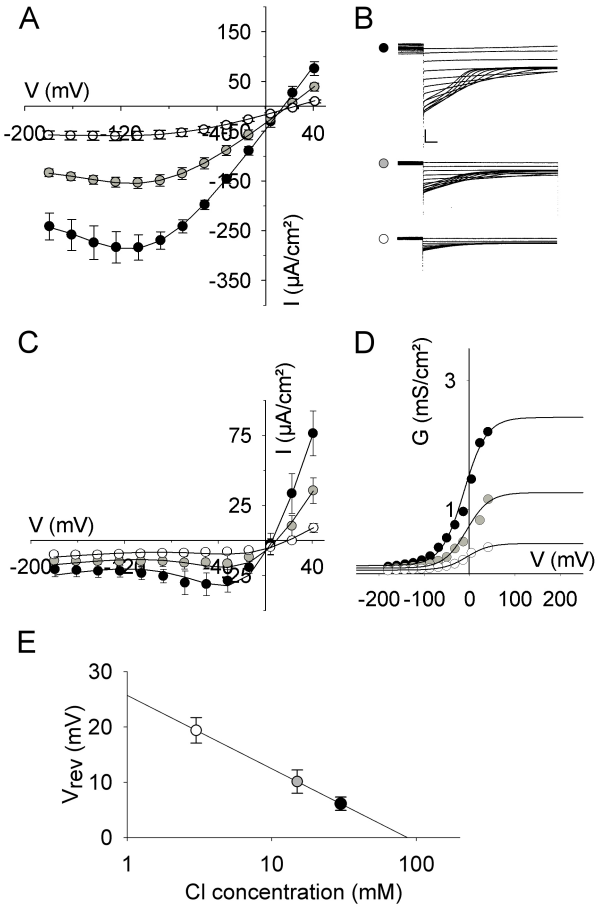

nph_16640_f2.jpg

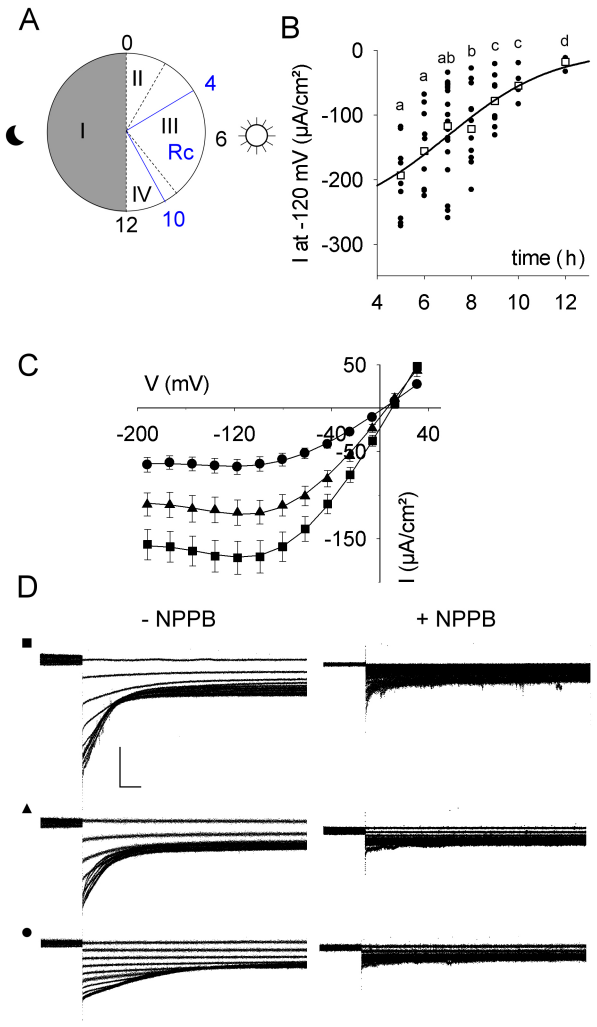

nph_16640_f3.jpg

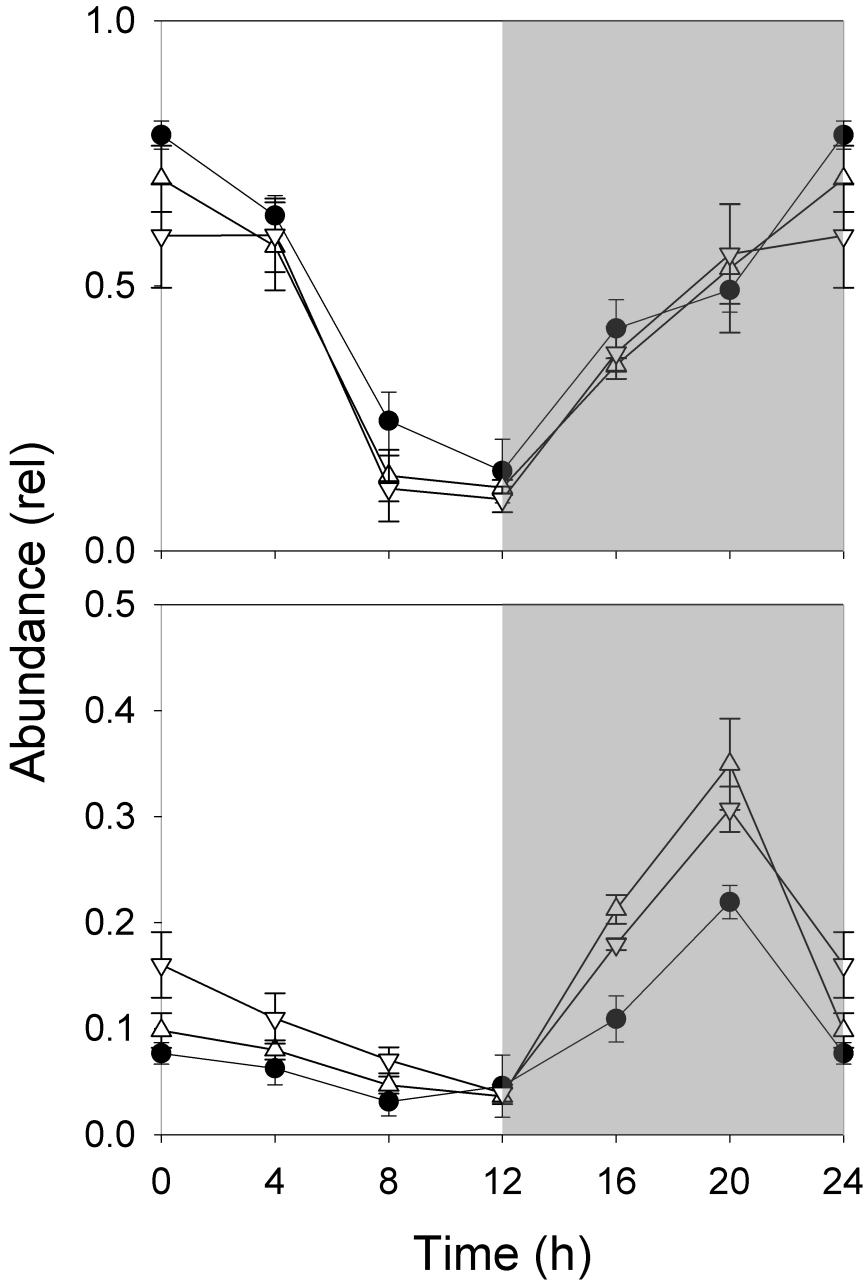

nph_16640_f4.jpg

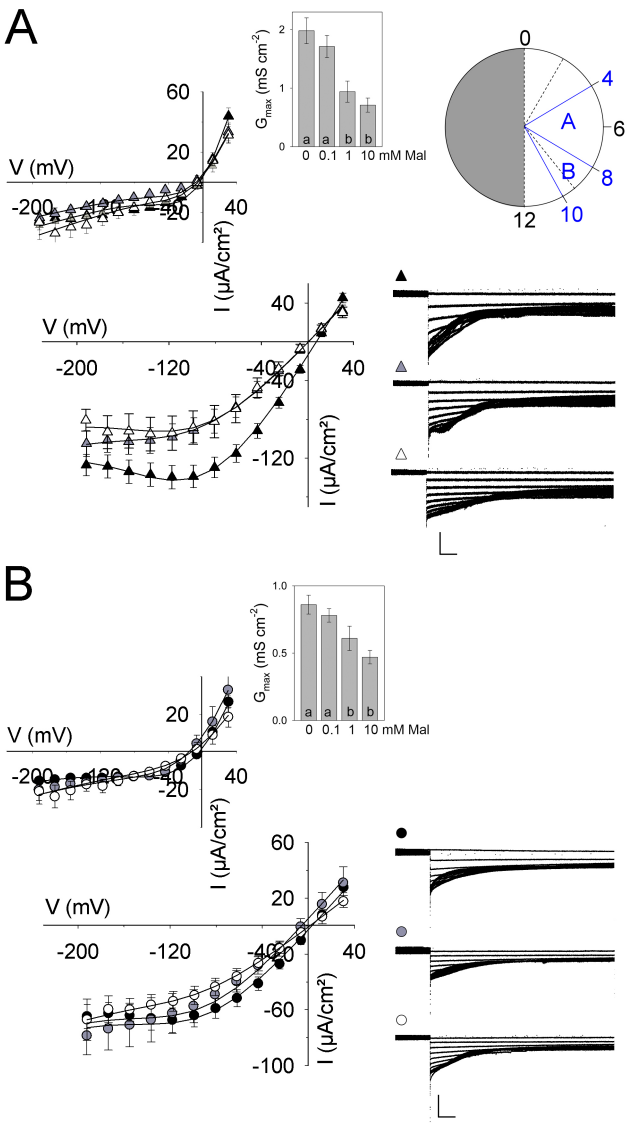

nph_16640_f5.jpg

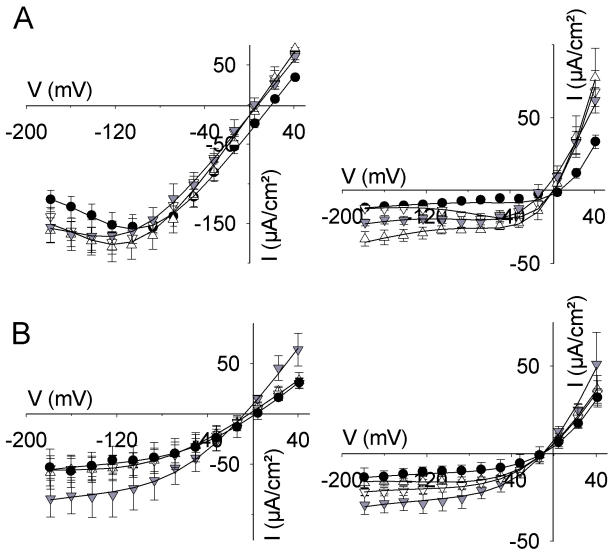

nph_16640_f6.jpg